

# Disappearance of the Telomere Dysfunction-Induced Stress Response in Fully Senescent Cells

Christopher J. Bakkenist, Rachid Drissi, Jing Wu, Michael B. Kastan, and Jeffrey S. Dome

Department of Hematology/Oncology, St. Jude Children's Research Hospital, Memphis, Tennessee

## Abstract

Replicative senescence is a natural barrier to cellular proliferation that is triggered by telomere erosion and dysfunction. Here, we demonstrate that ATM activation and H2AX- $\gamma$  nuclear focus formation are sensitive markers of telomere dysfunction in primary human fibroblasts. Whereas the activated form of ATM and H2AX- $\gamma$  foci were rarely observed in early-passage cells, they were readily detected in late-passage cells. The ectopic expression of telomerase in late-passage cells abrogated ATM activation and H2AX- $\gamma$  focus formation, suggesting that these stress responses were the consequence of telomere dysfunction. ATM activation was induced in quiescent fibroblasts by inhibition of TRF2 binding to telomeres, indicating that telomere uncapping is sufficient to initiate the telomere signaling response; breakage of chromosomes with telomeric associations is not required for this activation. Although ATM activation and H2AX- $\gamma$  foci were readily observed in late-passage cells, they disappeared once cells became fully senescent, indicating that constitutive signaling from dysfunctional telomeres is not required for the maintenance of senescence.

## Introduction

Primary human cells undergo a finite number of population doublings (PD), after which they assume a state of viable growth arrest called replicative senescence (1). The induction of replicative senescence is presumed to be related to telomere shortening and dysfunction because proliferative capacity correlates closely with telomere length (2) and because senescence can be averted with the ectopic expression of telomerase in a variety of cell types (3–5). Inactivation of the p53 and Rb pathways delays or bypasses senescence (6), suggesting that telomere dysfunction signals through these pathways to induce senescence.

Recent studies have demonstrated that telomere dysfunction activates a stress response that resembles a DNA damage response. Experiments in which telomeres were artificially “uncapped” by the inhibition of TRF2 binding have demonstrated that lymphocytes undergo apoptosis in a p53- and ATM-dependent manner and fibroblasts undergo senescence in a p53- and Rb-dependent manner (7, 8). Moreover, TRF2 inhibition resulted in the formation of telomeric foci containing activated ATM and other DNA damage response factors (9). These foci were diminished in response to treatment with caffeine and wortmannin, suggesting that PI3 kinases participate in telomere dysfunction-induced signaling (9). The documentation of H2AX- $\gamma$ , 53BP1, MDC1, NBS1, and SMC1–966S-P foci in senescing human fibroblasts indicated that a telomere dysfunction-induced stress re-

sponse may also be activated as a consequence of natural telomere shortening (10).

Although a telomere dysfunction-induced stress response becomes activated in senescing cells, it is unknown whether continued signaling persists into senescence. In the present study, we demonstrate that ATM activation, H2AX- $\gamma$  focus formation, and p53 accumulation increase in late-passage presenescent cells. However, once cells become fully senescent, these molecular markers of dysfunctional telomeres disappear. These results are consistent with the idea that constitutive signaling from dysfunctional telomeres is not required for the maintenance of senescence.

## Materials and Methods

**Cell Culture.** The 1070SK primary human foreskin fibroblast (HFF), IMR-90 primary human lung fibroblast, and the HeLa human cervical carcinoma cell lines were obtained from the American Type Culture Collection. 293T cells were a gift from Dr. David Baltimore (California Institute of Technology, Pasadena, CA). 1070SK and 293T cells were cultured in DMEM (Biowhittaker) supplemented with 10% fetal bovine serum (HyClone), L-glutamine, and penicillin/streptomycin (Life Technologies). IMR-90 cells were cultured in MEM Eagle medium (American Type Culture Collection) and 10% serum. Cells were propagated at 37°C and 5% CO<sub>2</sub> in a humidified incubator.

**Analysis of Senescence.** Senescence was assessed by staining for senescence-associated  $\beta$ -galactosidase (SA- $\beta$ -gal), as described previously (11). Bromodeoxyuridine (BrdUrd) incorporation was measured by incubating cells in the presence of BrdUrd for 24 h, followed by staining with anti-BrdUrd FITC-conjugated mouse monoclonal antibody (BD Bioscience) and propidium iodide and quantitation by fluorescence-activated cell sorting.

**Generation of Retroviruses and Lentiviruses.** For retrovirus generation, plasmids containing human telomerase reverse transcriptase (TERT) cDNA (pCI-neo-hEST2) were obtained from Dr. R. Weinberg (Whitehead Institute). TERT cDNA was subcloned into the retroviral expression vector MSCV-IGFP, which expresses the green fluorescent protein reporter from an internal ribosomal entry site. Vesicular stomatitis virus-G-pseudotyped retroviruses were packaged in 293T cells transfected with the plasmids pEQ-PAM3-E (containing the helper proteins), vesicular stomatitis virus-G (containing the envelope), and MSCV-IGFP or MSCV-IGFP-TERT. Virus-containing medium was applied to the cells of interest in three separate aliquots with Polybrene. Forty-eight h after transduction, green fluorescent protein-containing cells were isolated by fluorescence-activated cell sorting. For lentivirus generation, plasmids containing TRF2<sup>ABAM</sup> and TRF2<sup>AB</sup> were obtained from Dr. T. de Lange (Rockefeller University). Vesicular stomatitis virus-G-pseudotyped lentivirus were packaged in 293T cells transfected with the plasmids CAG vesicular stomatitis virus-G (envelope), CAG kGP1-RRE (gag/pol), CAG RTR2 (rev/tat), and vector plasmid (containing either TRF2<sup>AB</sup> or TRF2<sup>ABAM</sup>, LTR, and packaging signal), as described previously (12, 13). Virus-containing medium was applied to quiescent cells in two separate aliquots with Polybrene. Forty-eight h after transduction, ATM was immunoprecipitated from the cells and assessed by Western blotting.

**Telomerase Activity and Telomere-Length Assays.** Cell extracts were prepared according to protocols provided by the manufacturers. Telomerase activity was measured using the TRAPeze telomerase detection kit (Intergen). For telomere-length analysis, 5  $\mu$ g of genomic DNA were digested with *HinfI* and *RsaI* and analyzed by southern blotting using a <sup>32</sup>P-labeled (TTAGGG)<sub>6</sub>

Received 2/10/04; revised 3/24/04; accepted 4/8/04.

**Grant support:** NIH Grants CA71387 and CA21765 and the American Lebanese Syrian Associated Charities of St. Jude Children's Research Hospital.

The costs of publication of this article were defrayed in part by the payment of page charges. This article must therefore be hereby marked *advertisement* in accordance with 18 U.S.C. Section 1734 solely to indicate this fact.

**Note:** C. Bakkenist and R. Drissi contributed equally to this work.

**Requests for reprints:** Jeffrey S. Dome, St. Jude Children's Research Hospital, 332 North Lauderdale Street, Memphis, TN 38105. Phone: (901) 495-2533; Fax: (901) 495-3966; E-mail: jeff.dome@stjude.org.

probe. Signals were visualized using a Storm 860 PhosphorImager (Molecular Dynamics).

**Immunoprecipitation and Western Blotting.** Immunoprecipitation of ATM was performed as described previously (14). In brief, cells were scraped from flasks and lysed on ice for 20 min. Lysates were centrifuged at  $13,000 \times g$  for 15 min at  $4^{\circ}\text{C}$ . Supernatants were immunoprecipitated with anti-ATM D1611 (15) and protein A/G-agarose beads. The pelleted beads were washed once with lysis buffer and two to three times with radioimmunoprecipitation assay buffer. The immunoprecipitates were separated on SDS-PAGE and electroblotted onto nitrocellulose membrane. The membranes were incubated with anti-ATM MAT3 (gift of Dr. Y. Shiloh) or polyclonal anti-ATM 1981S-P. Immunoblots of soluble cell lysates were performed with Ab-6 (anti-p53, Oncogene Research Products), C-19 (anti-p21, Santa Cruz Biotechnology), and anti-TRF2 antibodies (Upstate Biotechnology).

**Immunofluorescence.** Monoclonal anti-ATM 1981S-P antisera was generated by immunizing mice with the keyhole limpet hemocyanin-conjugated synthetic peptide SLAFEEGSpQSTTIS (Rockland Immunochemicals). Fusion with Sp2/0 mouse myeloma cells generated a hybridoma (10H11.E12) that produced an IgG1/ $\kappa$  antibody specific for phosphorylated human ATM in Western blotting, immunoprecipitation, and immunofluorescence. Cells were seeded onto glass slides, cultured overnight, and fixed in 50% methanol/50% acetone for 1 h at  $-20^{\circ}\text{C}$ . The samples were blocked in PBS containing 10% FBS for 1 h at room temperature then incubated for 1 h at room temperature with primary antibodies anti-H2AX $\gamma$  at 1:500 dilution (Upstate Biotechnology) or with monoclonal anti-ATM 1981S-P at 1:20 dilution. The samples were then incubated for 1 h at room temperature with secondary antibodies antimouse-FITC at 1:125 dilution or with antirabbit-rhodamine at 1:250 dilution (Santa Cruz Biotechnology). The statistical comparison of foci in early-passage *versus* late-passage cells was performed using Fisher's exact test (GraphPad Prism).

## Results and Discussion

**ATM Activation Is a Marker of Telomere Dysfunction in Aging Human Fibroblasts.** ATM, the product of the gene that is mutated in the disorder ataxia telangiectasia, plays a critical role in the initiation of response pathways to ionizing radiation (IR). ATM exists as an inert homodimer in cells with undamaged DNA (14). In response to various types of DNA damage, ATM undergoes an intermolecular autophosphorylation on 1981S, leading to dimer dissociation, activa-

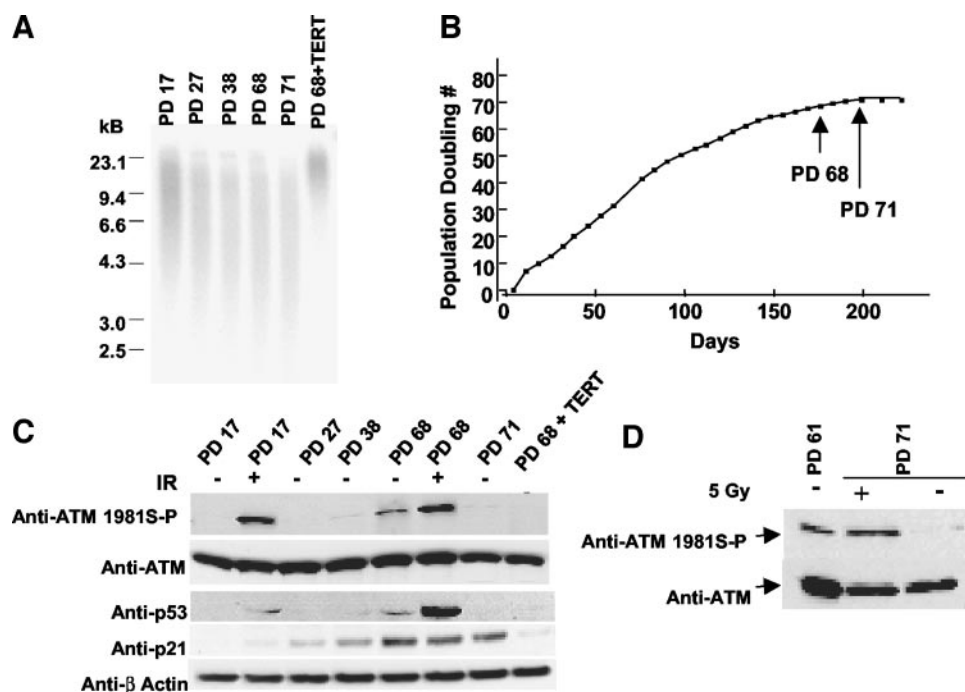
tion, and phosphorylation of downstream substrates. We used antibodies that specifically recognize ATM when it is phosphorylated on 1981S (1981S-P) to dissect the status of ATM activation during the establishment of replicative senescence.

We passaged 1070SK HFFs in culture over several months and assessed cells at different PD for signs of telomere dysfunction and ATM activation. As predicted, the cells underwent progressive telomere attrition (Fig. 1A). After 70 PD, cells stopped proliferating completely and became large and flat (Fig. 1B; data not shown). Immunoprecipitation of total ATM protein followed by immunoblotting with antibodies directed against total ATM or antibodies specific for ATM phosphorylated on 1981S revealed that levels of phosphorylated ATM increased progressively as the PD number increased to 68 doublings, whereas total ATM levels remained constant (Fig. 1, C and D). This ATM activation was accompanied by accumulation of p53 and p21, consistent with induction of the p53 pathway (Fig. 1C).

To confirm that ATM phosphorylation in late-passage fibroblasts resulted from telomere dysfunction and not the accumulation of other types of DNA damage, we transduced fibroblasts at PD 68 with a retroviral vector that expresses the catalytic component of human TERT. Transduced cells exhibited telomerase activity (data not shown) and elongated telomeres (Fig. 1A). Ectopic telomerase expression in late-passage cells abrogated ATM activation (Fig. 1C), demonstrating that the ATM activation observed in late-passage cells was a direct consequence of telomere dysfunction. These results corroborate studies of experimentally uncapped telomeres, which demonstrated the involvement of ATM in the cellular response to telomere dysfunction. In one study, TRF2 inhibition was shown to induce apoptosis in human B-cell lines in an ATM-dependent manner (7). In a subsequent study, TRF2 inhibition resulted in the formation of telomeric foci containing activated ATM and other DNA damage response factors (9). Such foci were diminished in response to treatment with caffeine and wortmannin, suggesting that PI3 kinases participate in telomere dysfunction-induced signaling (9).

**Telomere Uncapping Is Sufficient to Activate ATM.** Telomere dysfunction in aging cells creates two distinct molecular lesions that could potentially activate ATM: the uncapping itself and the chromo-

Fig. 1. ATM is activated in late-passage primary HFFs. A, telomere shortening in HFFs at different PD, as shown by this telomere-specific Southern blot. PD 68 + TERT represents HFFs that were transduced with TERT-expressing retrovirus at PD 68. B, kinetics of HFF growth. The cultures were passaged at 7-day intervals; the total numbers of cells per culture were determined before redilution of the cells to 1:10 per 75-cm<sup>2</sup> flask for repassage. C, ATM phosphorylation on 1981S upon telomere shortening. Whole-cell extracts were prepared from HFFs at the indicated PD. For irradiated HFFs, the extracts were prepared 1 h after 5-Gy irradiation. Cleared supernatants were immunoprecipitated with anti-ATM, and the samples were resolved by gel electrophoresis and immunoblotted with anti-ATM-1981S-P. A portion of the extracts from each sample was analyzed by immunoblot using antibodies directed against p53 and p21. D, ATM is not activated in senescent HFFs but retains the ability to be activated upon IR-induced DNA damage. Whole-cell extracts were prepared from senescent HFFs (PD 71), presenescent HFFs (PD 61), and HFFs at PD 71, 1 h after irradiation with 5 Gy. ATM was immunoprecipitated and immunoblotted with anti-ATM-1981S-P and anti-ATM.



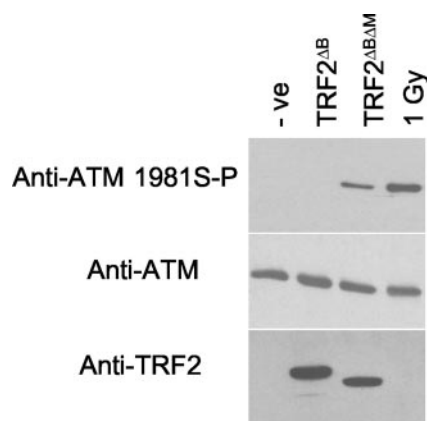


Fig. 2. ATM is phosphorylated in quiescent primary fibroblasts after transduction with dominant-negative TRF2.  $G_0$  primary fibroblasts were transduced with lentivirus expressing either TRF2<sup>ΔB</sup> or TRF2<sup>ΔBΔM</sup>. Forty-eight h later, ATM was immunoprecipitated and immunoblotted with anti-1981S-P or anti-ATM. The soluble cell extract was immunoblotted for TRF2. Full-length endogenous TRF2 was below the detection limit using these conditions. As a control for ATM phosphorylation, cells were assessed 30 min after IR (1 Gy).

some breakage that arises from dicentric chromosome rupture. To ascertain whether telomere-related ATM activation requires fusion-bridge-breakage cycles, we needed to disrupt telomere structure in the absence of cell cycle progression. Toward this end, we generated lentiviruses that express a dominant-inhibitory form of TRF2 (TRF2<sup>ΔBΔM</sup>), which is known to interfere with native TRF2 binding at telomeres and to elicit a telomere damage response (7, 16). As a control, we generated lentiviruses that express TRF2<sup>ΔB</sup>, a truncated form of TRF2 that does not behave in a dominant-negative fashion (7). The TRF2<sup>ΔBΔM</sup>- and TRF2<sup>ΔB</sup>-expressing lentiviruses were used to transduce contact-inhibited fibroblasts, which were demonstrated to be quiescent by the absence of incorporation of tritiated thymidine (data not shown). Transduction with TRF2<sup>ΔBΔM</sup>- and TRF2<sup>ΔB</sup>-expressing lentiviruses into quiescent cells yielded similar levels of protein expression detected by immunoblotting (Fig. 2). Immunoprecipitation with total ATM antibody followed by immunoblotting with the polyclonal anti-ATM 1981S-P revealed that ATM was phosphorylated in response to transduction with TRF2<sup>ΔBΔM</sup>, but not TRF2<sup>ΔB</sup>.

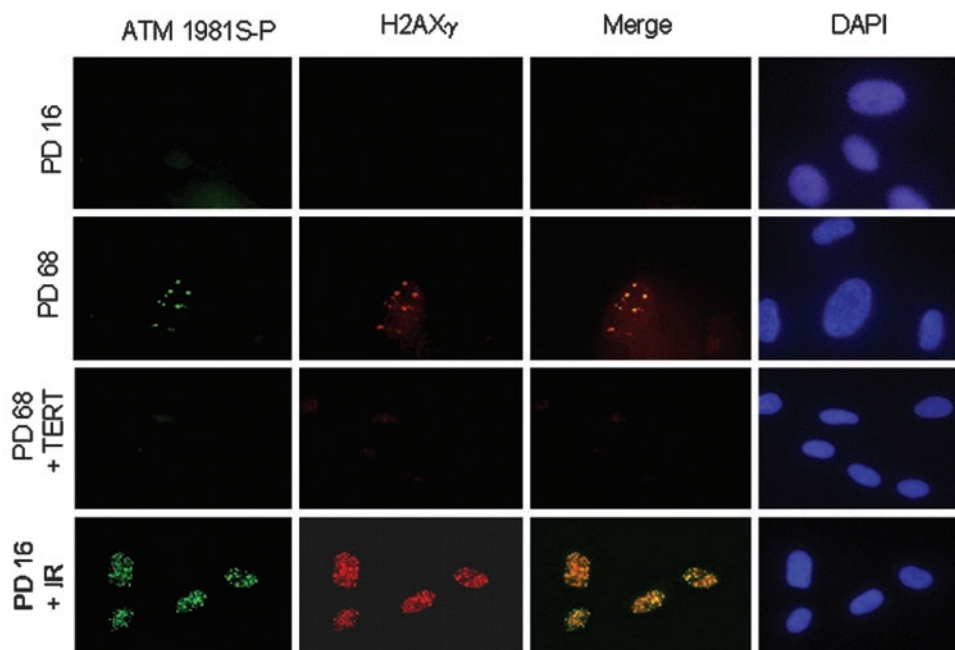
Because the cells were not cycling, this result indicates that neither mitosis nor passage through S phase are required to induce a telomere dysfunction-induced stress response. These results are consistent with the previous observations that cells undergo apoptosis in response to TRF2 inhibition before commencing S phase and that synchronized cells accumulate DNA damage foci before undergoing mitosis (7, 9).

**Accumulation of Nuclear Foci in Late-Passage Fibroblasts.** We next evaluated the localization of activated ATM in late-passage fibroblasts by immunofluorescence microscopy. For these experiments, we generated a new monoclonal antibody directed against ATM 1981S-P that exhibits very low levels of background staining. We observed that most early-passage fibroblasts did not show ATM staining, whereas late-passage fibroblasts frequently exhibited ATM staining that localized to nuclear foci (Fig. 3). As the cells were passaged, a progressive increase in the number of cells with at least three ATM 1981S-P foci was observed: 8% at PD 16; 15% at PD 35; 23% at PD 54; and 32% at PD 68 (32% versus 8%,  $P < 0.0001$ ). Notably, ATM foci were observed in fewer than 1% of late-passage fibroblasts with ectopic TERT expression, suggesting that the ATM foci observed in 8% of the early-passage cells resulted from telomere dysfunction. Therefore, the detection of ATM 1981S-P foci appears to be a highly sensitive marker of telomere dysfunction.

To evaluate whether ATM 1981S-P foci in late-passage cells colocalize with other DNA damage response proteins, we stained cells with an antibody directed against the phosphorylated form of H2AX (H2AX- $\gamma$ ), which is believed to coincide with DNA double-stranded breaks. Like phosphorylated ATM, H2AX- $\gamma$  foci were uncommon in early-passage fibroblasts, but were readily detected in late-passage cells, confirming previous reports (10, 17). There was significant colocalization of H2AX- $\gamma$  foci with ATM foci (Fig. 3), although this colocalization was not complete and more cells contained ATM foci than H2AX- $\gamma$  foci. Late-passage fibroblasts also had a high frequency of NBS1 foci and 53BP1 foci that colocalized with ATM foci (data not shown).

**The Telomere Dysfunction-Induced Stress Response Is Not Activated in Senescent Cells.** Activated ATM and p53 accumulation were observed in cells at PD 68 but diminished markedly when cells were passaged to PD 71 and maintained in culture for several weeks (Fig. 1C). Several lines of evidence suggest that the key distinction

Fig. 3. Late-passage fibroblasts contain ATM 1981S-P and H2AX- $\gamma$  nuclear foci. Asynchronously growing HFFs at PD 16, PD 68, and PD 68 + TERT were processed for immunofluorescence using monoclonal anti-ATM 1981S-P and anti-H2AX- $\gamma$ . HFFs at PD 16 were irradiated with 5 Gy and analyzed 1 h after irradiation. Nuclei were identified by 4',6-diamidino-2-phenylindole (DAPI) staining.



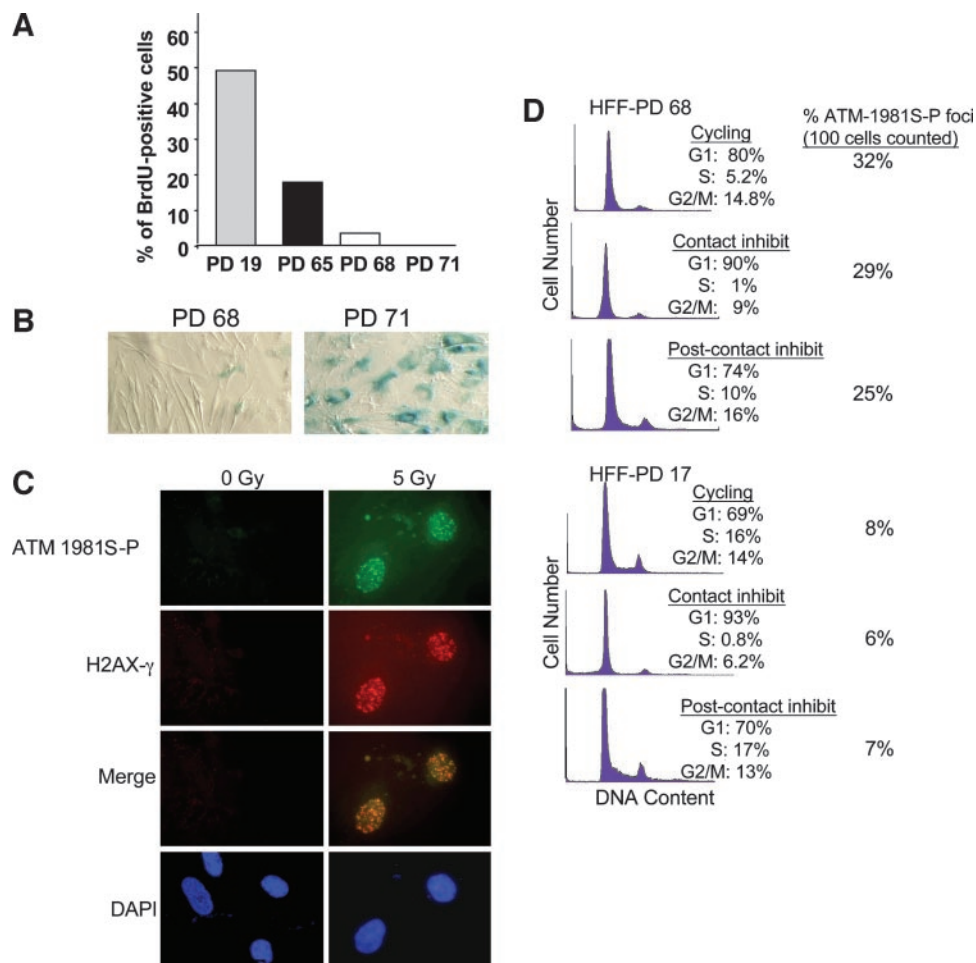


Fig. 4. ATM is not activated in senescent fibroblasts. **A**, BrdUrd incorporation decreases in late-passage HFFs and becomes undetectable by PD 71. **B**, SA- $\beta$ -gal expression in late-passage HFFs versus fully senescent fibroblasts. **C**, senescent HFFs at PD 71 were immunostained for ATM-1981S-P and H2AX- $\gamma$  before and 1 h after irradiation with 5 Gy. **D**, cycling HFFs, contact-inhibited HFFs, and HFFs 72 h post-release from contact inhibition at PD 17 and PD 68 were harvested for propidium iodide staining and fluorescence-activated cell sorting analysis. The histograms show that the percentage of cells with ATM 1981S-P foci remains unchanged whether or not the cells are cycling.

between these two populations of cells was that PD 68 cells were presenescent and PD 71 cells were fully senescent. First, PD 68 cells grew very slowly, whereas PD 71 cells did not proliferate at all (Fig. 1B). Second, 2–3% of PD 68 cells incorporated BrdUrd, whereas BrdUrd incorporation was not detectable beyond nonspecific background staining in PD 71 cells (Fig. 4A). Third, many PD 68 cells were small and spindle-shaped, whereas PD 71 cells were uniformly large and flat, representing a homogeneous population of senescent cells (Fig. 4B). Finally, only 5% of cells at PD 68 exhibited SA- $\beta$ -gal staining, which is considered to be a specific marker of senescence (11), whereas 98% of cells at PD 71 showed SA- $\beta$ -gal staining (Fig. 4B).

Although ATM was not constitutively activated in senescent cells, it had the ability to be activated in response to IR (Fig. 1D). This suggests that the short telomeres of senescent cells (as shown in Fig. 1A) are somehow shielded from initiating a signaling response. It has been shown that telomeres of senescent fibroblasts cannot be elongated with the ectopic expression of TERT, indicating that telomeres in senescent cells cannot be modified by telomerase (18). Perhaps the process that makes telomeres inaccessible to telomerase in senescent cells also prevents short telomeres from activating ATM. Additional studies are warranted to define the structural fate of telomeres post-senescence.

We extended the observation that ATM is not activated in senescent cells using immunofluorescence studies to detect ATM 1981S-P and H2AX- $\gamma$  foci in senescent cells. Unlike their predecessors at PD 68, senescent cells at PD 71 did not have detectable DNA damage response foci in the absence of IR (Fig. 4C). After 5-Gy IR, however,

PD71 cells readily formed such DNA damage response foci (Fig. 4C). To assess whether the disappearance of ATM activation in senescent cells is specific to the 1070SK fibroblast line, we repeated these experiments using the IMR-90 lung fibroblast line. As seen with the 1070SK cells, ATM was phosphorylated in late-passage but not senescent, IMR-90 cells (data not shown).

To ascertain whether the lack of ATM phosphorylation in senescent cells is specific to properties of senescence or is more generally related to lack of cell cycling, we arrested cell growth in early- and late-passage cells by contact inhibition. In this experiment, cells were contact-inhibited for 3 weeks past the point of confluence to maximize growth cessation and to allow baseline ATM 1981S-P foci to dissipate. At both early- and late-passages, the percentage of cells with ATM foci was unchanged whether or not the cells were quiescent (Fig. 4D). Notably, 25% of late-passage quiescent cells contained ATM foci, indicating that the absence of ATM activation in senescent cells cannot be accounted for solely by cell growth arrest.

Our observations contrast with the findings of other groups that senescent cells display H2AX- $\gamma$  foci (10, 17). We suspect that the previously described senescent cells were in the early stages of senescence, whereas our senescent cells were more deeply senescent. Because the telomere-dysfunction-induced stress response did not persist throughout senescence, we conclude that such a response is not required to maintain senescence. Recent studies have revealed that introduction of proteins that interfere with p53 function were able to induce DNA replication, and in the absence of up-regulated p16, cell proliferation in senescent cells (18, 19). This indicates that p53 contributes to the maintenance of senescence. Because we found that

the telomere dysfunction-induced signaling response is inactive in senescent cells, other factors must be responsible for maintaining p53 functionality in the senescent state.

In summary, our results indicate that telomere dysfunction-induced signaling pathways are engaged in senescing, but not senescent, fibroblasts. Our results are consistent with the idea that telomere erosion and dysfunction are critical inducers of senescence, but that once the senescence program is evoked, telomere signaling is no longer required to maintain senescence. Additional elucidation of the pathways that induce and maintain senescence will provide a greater understanding of the processes of aging and malignant transformation.

### Acknowledgments

We thank C. Bockhold and D. Woods for expert technical assistance. We thank D. Persons, P. Hargrove, and E. Vanin for assistance in generating the lentiviruses and retroviruses. We acknowledge T. de Lange, R. Weinberg, Y. Shiloh, and D. Baltimore for providing reagents.

### References

1. Campisi J. Cellular senescence as a tumor-suppressor mechanism. *Trends Cell Biol* 2001;11:S27–31.
2. Allsopp RC, Vaziri H, Patterson C, et al. Telomere length predicts replicative capacity of human fibroblasts. *Proc Natl Acad Sci USA* 1992;89:10114–8.
3. Bodnar AG, Ouellette M, Frolkis M, et al. Extension of life-span by introduction of telomerase into normal human cells. *Science* 1998;279:349–52.
4. Vaziri H, Benchimol S. Reconstitution of telomerase activity in normal human cells leads to elongation of telomeres and extended replicative life span. *Curr Biol* 1998; 8:279–82.
5. Herbert BS, Wright WE, Shay JW. p16(INK4a) inactivation is not required to immortalize human mammary epithelial cells. *Oncogene* 2002;21:7897–900.
6. Shay JW, Pereira-Smith OM, Wright WE. A role for both RB and p53 in the regulation of human cellular senescence. *Exp Cell Res* 1991;196:33–9.
7. Karlseder J, Broccoli D, Dai Y, Hardy S, de Lange T. p53-and ATM-dependent apoptosis induced by telomeres lacking TRF2. *Science* 1999;283:1321–5.
8. Smogorzewska A, de Lange T. Different telomere damage signaling pathways in human and mouse cells. *EMBO J* 2002;21:4338–48.
9. Takai H, Smogorzewska A, de Lange T. DNA damage foci at dysfunctional telomeres. *Curr Biol* 2003;13:1549–56.
10. d'Adda di Fagagna F, Reaper PM, Clay-Farrace L, et al. A DNA damage checkpoint response in telomere-initiated senescence. *Nature* 2003;426:194–8.
11. Dimri GP, Lee X, Basile G, et al. A biomarker that identifies senescent human cells in culture and in aging skin in vivo. *Proc Natl Acad Sci USA* 1995;92:9363–7.
12. Hanawa H, Kelly PF, Nathwani AC, et al. Comparison of various envelope proteins for their ability to pseudotype lentiviral vectors and transduce primitive hematopoietic cells from human blood. *Mol Ther* 2002;5:242–51.
13. Persons DA, Hargrove PW, Allay ER, Hanawa H, Nienhuis AW. The degree of phenotypic correction of murine  $\beta$ -thalassemia intermedia following lentiviral-mediated transfer of a human  $\gamma$ -globin gene is influenced by chromosomal position effects and vector copy number. *Blood* 2003;101:2175–83.
14. Bakkenist CJ, Kastan MB. DNA damage activates ATM through intermolecular autophosphorylation and dimer dissociation. *Nature* 2003;421:499–506.
15. Alligood KJ, Milla M, Rhodes N, et al. Monoclonal antibodies generated against recombinant ATM support kinase activity. *Hybridoma* 2000;19:317–21.
16. van Steensel B, Smogorzewska A, de Lange T. TRF2 protects human telomeres from end-to-end fusions. *Cell* 1998;92:401–13.
17. Sedelnikova OA, Horikawa I, Zimonjic DB, Popescu NC, Bonner WM, Barrett JC. Senescing human cells and ageing mice accumulate DNA lesions with unrepairable double-strand breaks. *Nat Cell Biol* 2004;6:168–70.
18. Beausejour CM, Krtolica A, Galimi F, et al. Reversal of human cellular senescence: roles of the p53 and p16 pathways. *EMBO J* 2003;22:4212–22.
19. Gire V, Wynford-Thomas D. Reinitiation of DNA synthesis and cell division in senescent human fibroblasts by microinjection of anti-p53 antibodies. *Mol Cell Biol* 1998;18:1611–21.

# Cancer Research

The Journal of Cancer Research (1916–1930) | The American Journal of Cancer (1931–1940)

## Disappearance of the Telomere Dysfunction-Induced Stress Response in Fully Senescent Cells

Christopher J. Bakkenist, Rachid Drissi, Jing Wu, et al.

*Cancer Res* 2004;64:3748-3752.

**Updated version** Access the most recent version of this article at:  
<http://cancerres.aacrjournals.org/content/64/11/3748>

**Cited articles** This article cites 19 articles, 8 of which you can access for free at:  
<http://cancerres.aacrjournals.org/content/64/11/3748.full#ref-list-1>

**Citing articles** This article has been cited by 7 HighWire-hosted articles. Access the articles at:  
<http://cancerres.aacrjournals.org/content/64/11/3748.full#related-urls>

**E-mail alerts** [Sign up to receive free email-alerts](#) related to this article or journal.

**Reprints and Subscriptions** To order reprints of this article or to subscribe to the journal, contact the AACR Publications Department at [pubs@aacr.org](mailto:pubs@aacr.org).

**Permissions** To request permission to re-use all or part of this article, use this link  
<http://cancerres.aacrjournals.org/content/64/11/3748>.  
Click on "Request Permissions" which will take you to the Copyright Clearance Center's (CCC) Rightslink site.